

Differential Regulation of Cancer Progression by CDK4/6 Plays a Central Role in DNA Replication and Repair Pathways



Meiou Dai¹, Julien Boudreault¹, Ni Wang¹, Sophie Poulet¹, Girija Daliah¹, Gang Yan¹, Alaa Moamer¹, Sergio A. Burgos^{2,3}, Siham Sabri¹, Suhad Ali¹, and Jean-Jacques Lebrun¹

ABSTRACT

Although the cyclin-dependent kinases CDK4 and CDK6 play fundamental roles in cancer, the specific pathways and downstream targets by which they exert their tumorigenic effects remain elusive. In this study, we uncover distinct and novel functions for these kinases in regulating tumor formation and metastatic colonization in various solid tumors, including those of the breast, prostate, and pancreas. Combining *in vivo* CRISPR-based CDK4 and CDK6 gene editing with pharmacologic inhibition approaches in orthotopic transplantation and patient-derived xenograft preclinical models, we defined clear functions for CDK4 and CDK6 in facilitating tumor growth and progression in metastatic cancers. Transcriptomic profiling of CDK4/6 CRISPR knockouts in breast cancer revealed these two kinases to regulate cancer progression through distinct mechanisms. CDK4 regulated prometastatic inflammatory cytokine signaling,

whereas CDK6 mainly controlled DNA replication and repair processes. Inhibition of CDK6 but not CDK4 resulted in defective DNA repair and increased DNA damage. Multiple CDK6 DNA replication/repair genes were not only associated with cancer subtype, grades, and poor clinical outcomes, but also facilitated primary tumor growth and metastasis *in vivo*. CRISPR-based genomic deletion of CDK6 efficiently blocked tumor formation and progression in preestablished cell- and patient-derived xenograft preclinical models of breast cancer, providing a potential novel targeted therapy for these deadly tumors.

Significance: In-depth transcriptomic analysis identifies cyclin-dependent kinases CDK4 and CDK6 as regulators of metastasis through distinct signaling pathways and reveals the DNA replication/repair pathway as central in promoting these effects.

Introduction

The cell-cycle and DNA replication processes are tightly coordinated to ensure proper single genome duplication in each cell division. Cyclin-dependent kinases (CDK) play a central role in coordinating cell-cycle transitions and DNA replication. CDK4 and CDK6 are key G₁ phase regulators that govern entry into the cell cycle (1). Upon mitogenic stimulation, the G₁ phase is triggered by the release of the INK4 inhibitor from the cyclin D–CDK4/6 complex, leading to phosphorylation of the retinoblastoma (RB) protein and further activation of the cell proliferation E2F transcriptional program (2). During G₁ to S-phase transition, the CDK2/cyclin E complex also leads to activation of the helicase minichromosome maintenance complex and initiation of DNA synthesis (3). DNA replication is the most vulnerable cellular process targeted by oncogenic insults and oncogene-induced DNA replication stress has been indicated as a driver of tumorigenesis (4).

While in normal cells, the cell cycle can progress in the absence of cyclin Ds or CDK4/6 (5, 6), cancer cells are dependent on increased cyclin D expression and hyperactive CDK4/6 for their proliferation (7, 8). In fact, genetic events that modulate expression and/or activation of the cell-cycle regulators are frequent in cancer, leading to tumor development and progression (9). Furthermore, hyperactivation of the cyclin D1/CDK4 complex is the ultimate downstream target for many oncogenic events such as HER2- and RAS-induced primary tumor growth in breast cancer and non-small cell lung carcinoma (5, 10–12). Although CDK4 and CDK6 are highly homologous, genomic analysis of patient tumor samples suggested certain cancers exhibit a more selective dependency toward CDK4 or CDK6. Indeed, CDK4 deregulation is more often found in epithelial tumors, such as those from the breast, skin, and lung tissues (13). In contrast, CDK6 hyperactivity is more common in mesenchymal malignancies, such as lymphoid leukemias and sarcomas (14). This tumor type specificity for CDK4 and CDK6 suggests that the two closely related kinases exhibit distinct functions and specific gene signatures. In support of this notion, aside from their canonical substrate RB, more than one hundred proteins have been found to be phosphorylated by these two kinases, with a much broader spectrum for CDK6 (15).

Newly uncovered cell-cycle-independent functions for cyclin D1/CDK4 on cancer cell migration, epithelial-to-mesenchymal transition and cancer stem cell (CSC) self-renewal suggest that these kinases may also contribute to tumor progression and metastases (16–18). Consistent with this possibility, palbociclib, a CDK4/6 inhibitor (CDK4/6i), was found to reduce metastatic burden in an orthotopic patient-derived xenograft mouse model of breast cancer (19). Moreover, we recently found that blocking CDK4/6 activity using palbociclib efficiently reduced CSC numbers and reversed the phenotype from mesenchymal to an epithelial/luminal-like in triple-negative breast cancer (TNBC; ER/PR/HER negative) cells, correlating with better

¹Department of Medicine, McGill University Health Center, Cancer Research Program, Montreal, Quebec, Canada. ²Department of Animal Science, McGill University, Sainte-Anne-de-Bellevue, Canada. ³Department of Medicine, McGill University Health Center, Metabolic Disorders and Complications Program, Montreal, Quebec, Canada.

Note: Supplementary data for this article are available at Cancer Research Online (<http://cancerres.aacrjournals.org/>).

J. Boudreault and N. Wang contributed equally to this article.

Corresponding Author: Jean-Jacques Lebrun, McGill University Health Center, 1001 Decarie Blvd, Block E, Suite E02.6224, Montreal, Quebec H4A 3J1, Canada. Phone: 514-934-1934, ext. 34846; E-mail: JJ.Lebrun@mcgill.ca

Cancer Res 2021;81:1332–46

doi: 10.1158/0008-5472.CAN-20-2121

©2020 American Association for Cancer Research.

patient prognosis and clinical outcomes (18). These studies suggest that, in addition to promoting tumorigenesis, CDK4/6 may also regulate the metastatic process. To date, several CDK4/6i have been approved for treatment of ER⁺ metastatic breast cancer in combination with aromatase inhibitors or ER antagonists (20). However, an early single-arm trial of palbociclib in RB-positive metastatic breast cancer showed that the single-agent palbociclib is more effective in HR⁺ than HR⁻ TNBC patients (21). It is worth noting that only four patients with TNBC were enrolled in this trial, highlighting the need for further trials with better patient stratification and larger cohorts. Therefore, it is critical to better understand the function of CDK4/6 in metastatic TNBC and to identify their downstream effectors on tumor initiation and progression.

In this study, we characterized the CDK4- and CDK6-specific transcriptomes to further define their function to primary tumor formation and metastasis in the context of different solid tumor types. To this end, we used clustered regularly interspaced short palindromic repeats knockout (CRISPR-KO) CDK4/6 cancer models and high-throughput gene profiling, large cancer patient datasets, and bioinformatic analysis as well as multiple preclinical mouse models of cancer. We found that blocking CDK4/6 expression using CRISPR-KO efficiently inhibited cancer growth and metastatic colonization to distant organs in multiple solid tumor types including breast, prostate, and pancreas. Interestingly, we found that CDK4 and CDK6 regulate distinct gene sets and pathways to mediate these tumorigenic effects. Pathway enrichment analysis of RNA-sequencing (RNA-seq) data revealed that CDK4 regulates prometastatic inflammatory pathways while CDK6 regulates genes involved in the DNA replication and repair processes. Importantly, we found that CDK6 deletion or its pharmacologic inhibition decreased expression of major homologous recombination DNA repair proteins and led to increased DNA damage. We further identified five major DNA replication and repair genes (*TK1*, *DTL*, *POLD3*, *POLE2*, and *CENPI*) as CDK6-specific transcriptional targets and uncovered new critical tumorigenic functions for these genes in mediating CDK6 effects. These results demonstrate the prominent role played by CDK6 and downstream DNA replication and repair genes in cancer growth and progression. From a therapeutic perspective, we also showed that intratumoral and intravenous *in vivo* delivery of a CRISPR/Cas9/CDK6 guide RNA (gRNA) using a clinical-grade polymer-based lipid reagent (*in vivo*-jetPEI) efficiently reduced primary tumor burden and metastatic colonization of the lungs, using cell- and patient-derived xenografts preclinical models of breast cancer.

Materials and Methods

Cell culture

SUM159PT cells were obtained from Stephen Ethier (The Medical University of South Carolina, Charleston, SC). MDAMB231, MDAMB468, PC3, and HPAF-II were obtained from the ATCC. HEK293T cells were obtained from GenHunter. All cells used were cultured at 37°C in 5% CO₂. HEK293T, MDA-MB-468, and MDA-MB-231 were maintained in DMEM (Wisent Bio) with 10% FBS (Gibco). SUM159PT was maintained in Ham F-12 media with 5% FBS, 5 µg/mL insulin, and 1 µg/mL hydrocortisone (Wisent Bio). HPAF-II was maintained in Eagle minimum essential medium (Wisent Bio) with 10% FBS. PC-3 was maintained in Ham F-12K medium with 10% FBS. All cell lines were used at early passage between 3 and 15 passages. All the cell lines were routinely tested by PCR kit for *Mycoplasma* by Diagnostic Laboratory from Comparative Medicine and Animal

Resources Centre (McGill University, Montreal, Quebec, Canada). All cell lines are *Mycoplasma* negative. All cell line authentication except SUM159 was performed by short tandem repeat profiling at ATCC.

CRISPR knockout plasmid cloning

The single vector system lentiCRISPR V2 backbone (Addgene, plasmid # 52961) was used to clone the nontargeting and targeting gRNA sequences for CDK4, CDK6, DTL, TK1, POLD3, HIST1H2BH, E2F8, PTN, LRIG3, PELI2, PIM1, PCNA, POLE2, and CENPI. Cloning was performed as described in the Addgene protocol (22). The three gRNAs for each gene each target different genomic regions and oligo sequences listed in Supplementary Table S1. Backbone vector was digested and dephosphorylated by *BsmBI* and FastAP (Fermentas) for 30 minutes at 37°C. The digested plasmid was gel-purified by QIAquick Gel Extraction Kit (Qiagen). The pair of oligos for each gene were phosphorylated and annealed using T4 PNK enzyme in a thermocycler by incubating 30 minutes at 37°C and 5 minutes at 95°C and ramp down to 25°C. Annealed oligos were diluted at 1:200 and ligated together with digested vector using Quick ligase (NEB) for 20 minutes at room temperature. The cloned vectors were then transformed into Stbl3 bacteria (Invitrogen).

Lentiviral production and infection

The HEK293T cell line was transfected for 16 hours at 37°C using 15 µg cloned vector for each gene, 4.5 µg pMD2.G (Addgene, 12259), and 12 µg psPAX2 (Addgene, 12260). The medium was then changed with fresh complete medium DMEM with 10% FBS. After 24-hour virus production, the medium was collected and centrifuged at 1,200 rpm for 5 minutes to remove any cells in the medium and the supernatant containing virus was collected. All cancer cell lines were then infected with 8 µg/mL of polybrene and 100 µL of virus for each plate overnight. Thirty-six hours postinfection, puromycin was added to all KO cells and cells were selected for at least 7 days.

For rescue CDK6, 2 µg HA-tagged CDK6 cDNA (Addgene, 1868; ref. 23) was transfected with Lipofectamine 3000 (Invitrogen) according to the manufacturer's protocol for 3 days.

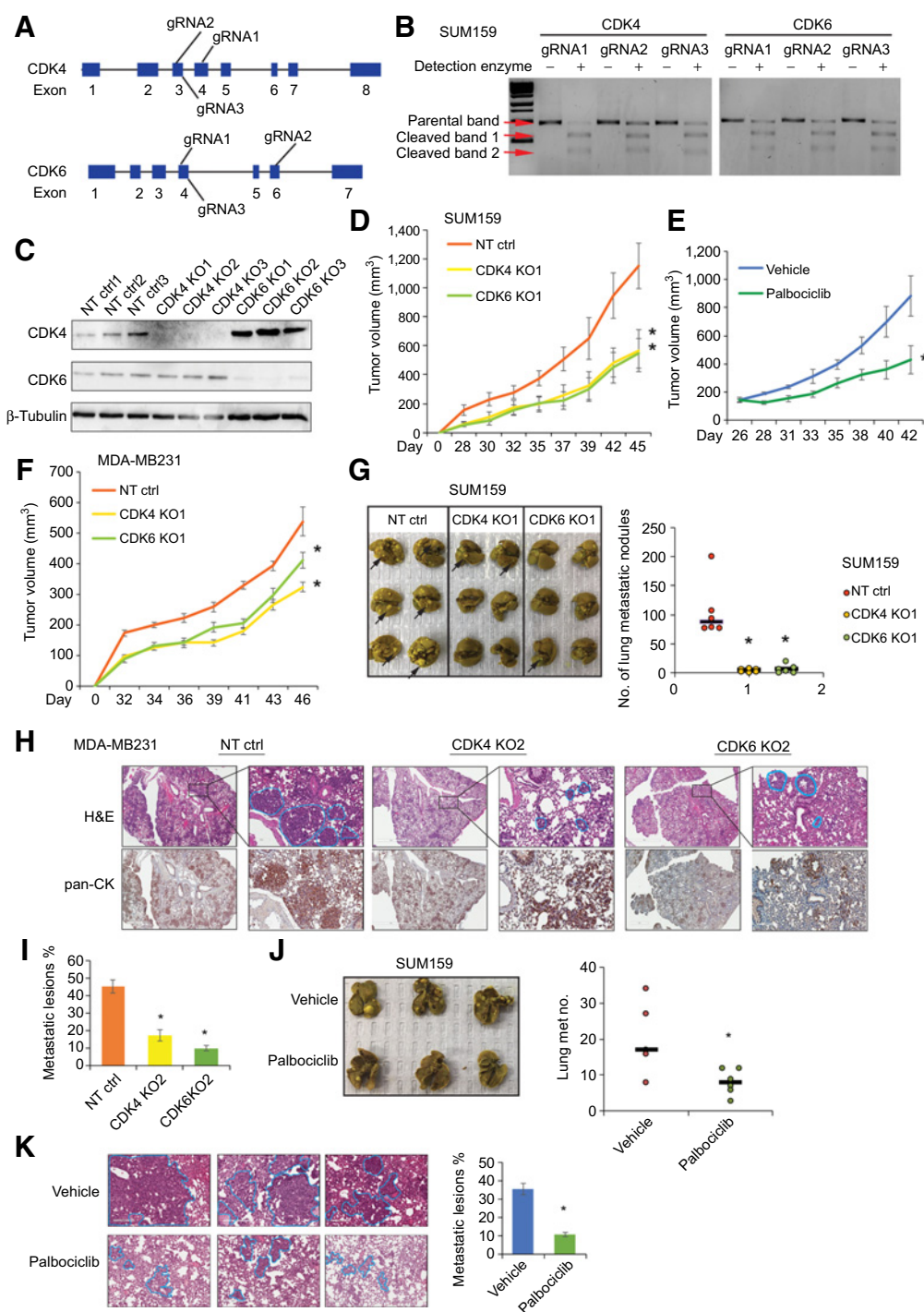
Genomic DNA cleavage assay

The genomic DNA cleavage assays for all genes were performed using GeneArt Genomic Cleavage Detection Kit (Invitrogen) according to the manufacturer's protocol. Briefly, 5 × 10⁵ of the stable KO cells were collected and genomic DNA was extracted. Primers were designed to amplify the specific loci modified by PCR. The primer sequences are listed in Supplementary Table S2. The PCR products containing the insertion/deletion, or mismatched DNA (indel) were then cleaved by the Detection Enzyme.

Immunoblotting

Total protein from the infected cells was extracted using ice-cold lysis buffer (50 mmol/L Tris-HCl, 150 mmol/L NaCl, 1% Triton X-100, 1 mmol/L EDTA, 100 mmol/L Na₃VO₄, protease inhibitors, phosphatase inhibitors). Cell lysates were then centrifuged at 12,000 rpm for 20 minutes at 4°C. The protein concentration for supernatant was determined using the BCA Kit (Thermo Fisher Scientific). The lysate samples were diluted in 5 × SDS Buffer and heated at 95°C for 5 minutes prior to loading on gel. Following electrophoresis, proteins were transferred onto nitrocellulose and blocked for 1 hour in 5% non-fat milk at room temperature. The membrane was then incubated

Dai et al.

**Figure 1.**

CDK4 and CDK6 CRISPR-KO impair primary tumor growth and metastatic colonization in TNBC cells. **A**, Three specific gRNAs targeting distinct genomic sites on each gene were generated and delivered through lentiviral infection. **B**, Gene modification of the CDK4 and CDK6 gRNAs were determined using genomic cleavage assays. **C**, CDK4 and CDK6 KO efficiency from three different gRNAs in breast cancer cells (SUM159) was assessed at the protein level by immunoblotting. **D**, The NT ctrl, CDK4 KO1, and CDK6 KO1 SUM159 cells were xenografted in NSG mice ($n = 8$ per group) through orthotopic mammary fat pad transplantation and primary tumor growth was assessed by measuring tumor volume. **E**, SUM159 cells were xenografted in NSG mice through mammary fat pad transplantation and allowed to develop for 26 days. Mice were then separated into two groups ($n = 7$ per group) with similar average tumor volume and treated daily with vehicle or palbociclib (30 mg/kg) by intraperitoneal injection. Primary mammary tumor growth was assessed by measuring tumor volume. **F**, MDA-MB-231 KO cells from gRNA1 ($n = 10$ mice per group) were xenografted through orthotopic mammary fat pad transplantation in NSG mice and primary tumor growth was assessed by measuring tumor volume. (Continued on the following page.)

overnight at 4°C with the primary antibodies (detailed information in Supplementary Table S3). Following 1-hour incubation with specific secondary antibodies, membranes were washed, and revealed by ECL using the ChemiDoc Touch Instrument (Bio-Rad).

Tumorsphere formation assay

NT and CDK4/6 KO SUM159 cells were seeded in 24-well low-attachment plate and incubated for 7 days in DMEM/F12 supplemented with B27, 10 ng/mL EGF, and 10 ng/mL bFGF and tumorsphere cell number were counted.

Cell viability

NT and CDK4/6 KO SUM159 cells were seeded (100 cells/well) in 96-well plates for 4 and 7 days and followed by incubation of 10% PrestoBlue Reagent (Thermo Fisher Scientific) at 37°C for 2 hours. Cell viability was measured by fluorescence (excitation/emission at 560/590 nm) using a plate reader.

Apoptosis assay

NT and CDK4/6 KO SUM159 cells were stained with Annexin V FITC and PI using Annexin V Apoptosis Detection Kit (Santa Cruz Biotechnology) for 15 minutes at room temperature according to the manufacturer's protocol. Percentage of Annexin⁺/PI⁻ (early apoptosis) and Annexin V⁺/PI⁺ (late apoptosis) was quantified by flow cytometry.

Immunofluorescence

SUM159 cells were fixed by ice-cold methanol for 15 minutes at -20°C. After blocking for 30 minutes in 2% BSA, cells were incubated with γ H2AX primary antibody and then secondary anti-Rabbit Alexa Fluor 568 (Invitrogen) for 1 hour at room temperature. The cells were then mounted on the microscope slides and scanned using the confocal microscope (Zeiss LSM780). Intensity of γ H2AX was quantified by ImageJ software.

IHC

Mouse lung tissues with metastatic nodules were fixed in 10% formalin for at least 24 hours. Lung tissues were embedded and section into 5 μ m per slide. The slides were then boiled with 10 mmol/L citrate buffer (pH 6.0) at 95°C for 15 minutes. The slides were stained with hematoxylin and eosin and pan-cytokeratin (Thermo Fisher Scientific, 1:200) for 1 hour to assess lung metastasis. Ki67 antibody was used to stain tumor tissue for 1 hour. HRP Polymer and DAB Plus Chromogen (Thermo Fisher Scientific) was used for detection. All images were scanned by ScanScope digital scanner (Aperio). Quantification of Ki67-positive tumor cells was performed using the ImageJ plugin ImmunoRatio (24).

In vivo studies

All mice were housed and handled in accordance to the approved guidelines of the Canadian Council on Animal Care and the Animal Care Committee of McGill University (AUP # 7497). The immune-deficient non-obese diabetic *scid* gamma (NSG) mouse breeders were purchased from The Jackson Laboratory.

Human breast cancer cells, SUM159 or MDA-MB-231 (1×10^6 /mouse), were diluted 1:1 with Matrigel and then inoculated in the mammary fat pads of 8-week-old, female NSG mice to generate breast cancer tumors. Tumor sizes were measured with a digital electronic caliper three times per week to reach maximum volume of 1,000 mm³ prior to euthanasia. To generate a growth curve, tumor volumes were calculated according to the following formula: $[4/3 \times \pi \times (\text{Length}/2) \times (\text{Width}/2)^2]$.

Both cell lines (1×10^6 cells of each) were injected by tail vein to allow for lung metastasis development. The mice were euthanized at the indicated times after injection. The lung tissues were counted for metastatic nodules post-Bouin solution fixation (SUM159) or fixed in 10% neutral buffered formalin solution before sectioning and H&E staining (MBA-MB-231).

Human pancreatic cancer cell line HPAFII (1×10^6 /mouse) was inoculated in 7-week-old male NSG mice by intra-pancreas route to generate pancreatic tumor (with Matrigel) or by intra-splenic injection to evaluate liver metastases formation. The mice were euthanized at the indicated time for measuring pancreas tumor size and counting metastatic nodules on the liver surface.

Human prostate cancer PC3 cells (1×10^6 /mouse) were injected through tail vein or subcutaneous routes. Tumor sizes were measured three times per week with a digital electronic caliper. The metastasis nodules on lung, liver and kidneys were counted at the indicated time.

RNA sequencing

RNA samples were extracted using TRIzol from CDK4 and CDK6KO SUM159 and nontargeted cells treated with or without 100 nmol/L palbociclib for 24 hours. RNA-seq was performed at the McGill Genome Quebec Centre using the Illumina HiSeq 4000 system. Paired-end 100 bp RNA-seq, 50 million reads per sample, were mapped to the GRCh38 assembly of human genome using HISAT2 (25), with default parameters. Mapped reads were sorted by read name using SAMTools (26). Gene annotations were obtained from Ensembl (27) version 85, and gene-level read counts were calculated using htseq-count from the HTSeq package (28). Only reads with MAPQ score ≥ 30 were used for read counting, including only those that map to gene annotations with the "intersection-strict" parameter of htseq-count.

Variance-stabilized transformation from DESeq2 (29) was used to estimate the logarithm of read abundances for each gene in each sample that were the basis for hierarchical clustering and principal component analyses plots. Hierarchical clustering was performed using complete link, based on Euclidean distance of gene expression profiles. DESeq2 was also used to identify differentially expressed genes in paired comparisons. Pathway enrichment analysis was performed using EnrichR. Upregulated and downregulated genes were analyzed separately for each analysis, genes with significant differential expression [fold change (FC) >1.5 , <-1.5 ; false discovery rate (FDR) < 0.05] were used for enrichment test.

In vivo CRISPR delivery

SUM159 cells (1×10^6) were injected into mammary fat pad of NSG mice to develop primary mammary tumor for 35 days. For each mouse,

(Continued.) **G**, NT, CDK4, and CDK6 KO SUM159 breast cancer cells were injected intravenously in NSG mice ($n = 6$ per group) to assess the number metastatic nodules in the lungs. Data are represented as dot plots for individual mice. The midlines show median value. Representative images of metastatic nodules are shown for each mouse's lungs. Arrows, metastatic nodules. **H** and **I**, NT, CDK4, and CDK6 KO MDA-MB-231 breast cancer cells were injected in the tail vein of NSG mice ($n = 4$) and lung metastasis was assessed by hematoxylin and eosin (H&E) staining and pan-cytokeratin (pan-CK) IHC. Blue lines delineate the metastatic lesions in the lung. The percentage of tumor area was measured. **J** and **K**, Lung metastatic nodules and area were quantified from mice ($n = 6$ per group) intravenously injected with SUM159 (**J**) and MDA (**K**) and treated with vehicle and palbociclib (30 mg/kg) treatment daily. All data are mean \pm SEM from three biological replicates unless otherwise stated. *, $P < 0.05$ by Student *t* test.

Dai et al.

10 µg of each CRISPR/Cas9 plasmid DNA construct expressing single NT gRNAs or gRNAs targeting CDK6, was diluted 1:1 with 10% glucose solution. 1.2 µL InvivoJet PEI (Polyplus) was diluted with 10 µL of 10% glucose and completed to 20 µL total with sterile water. Plasmids and InvivoJet PEI mixtures were then combined and incubated for 15 minutes at room temperature. The 40 µL plasmid complexes were then injected by intratumoral route at multiple sites two times per week for a total of two weeks.

For intravenous delivery, 1×10^6 SUM159 cells were first injected intravenously for 7 days. Forty micrograms of plasmid mixture in 100 µL volume was combined with 100 µL InvivoJet PEI mixture containing 6.4 µL InvivoJet PEI. The plasmid complexes were then delivered intravenously once per week for four weeks.

The TNBC patient-derived xenograft (PDX) model TM00096 was obtained from The Jackson Laboratory. Detailed patient information is available on the company's website. To expand PDX primary tumor in NSG mice, tumor tissues were minced and subcutaneously transplanted into recipient mice. Tumor sizes were monitored with a digital electronic caliper and allowed to develop to approximately 200 mm³. Mice were separated into three groups (6 mice per group) based on similar average tumor size. Animals were subjected to the same dose of CRISPR/Cas9 gRNAs as intratumoral delivery twice per week for two weeks.

Statistical analyses

All results are presented as the mean \pm SEM for at least three repeated individual experiments unless otherwise stated. The difference between groups was analyzed using Student *t* test. A *P* < 0.05 was considered statistically significant.

Results

CDK4 and CDK6 CRISPR-KOs block primary tumor growth and metastatic colonization

To functionally characterize the role of CDK4 and CDK6 on primary tumor growth *in vivo*, we initially used two highly metastatic basal-like TNBC cell lines, SUM159 and MDA-MB-231 (herein referred to as MDA). CDK4 and CDK6 were selectively deleted in these cell lines using CRISPR/Cas9. Three specific gRNAs targeting distinct genomic loci on each gene were generated and delivered through lentiviral infection (Fig. 1A). On-target CRISPR-induced genomic editing was confirmed using DNA cleavage assay (Fig. 1B). Knockout efficiency was further assessed at the protein level by immunoblotting of CDK4 and CDK6 (Fig. 1C). CDK4 and CDK6 KO SUM159 cells were then transplanted into the mammary fat pads of NSG mice to assess orthotopic primary tumor growth. As shown in Fig. 1D and E, deletion of CDK4/6, or kinase inhibition by palbociclib, significantly reduced primary tumor growth compared to nontargeting control (NT ctrl) infected cells. These experiments were also performed in MDA cells and showed that primary tumor growth was significantly impaired in the absence of either CDK4 or CDK6 using two specific gRNAs for each gene (Fig. 1F; Supplementary Fig. S1).

To determine whether CDK4/6 could also regulate metastatic processes, CDK4 and CDK6 KO cells were injected intravenously into NSG mice. Interestingly, while mice injected with NT Ctrl developed high numbers of lung metastatic nodules after five weeks, deletion of either CDK4 or CDK6 in SUM159 cells completely prevented metastatic colonization of the lungs by the breast cancer cells (Fig. 1G). Similar results were obtained with the MDA CDK4/6 KO cells, as assessed by the percentage of tumor cells area within invasive lung

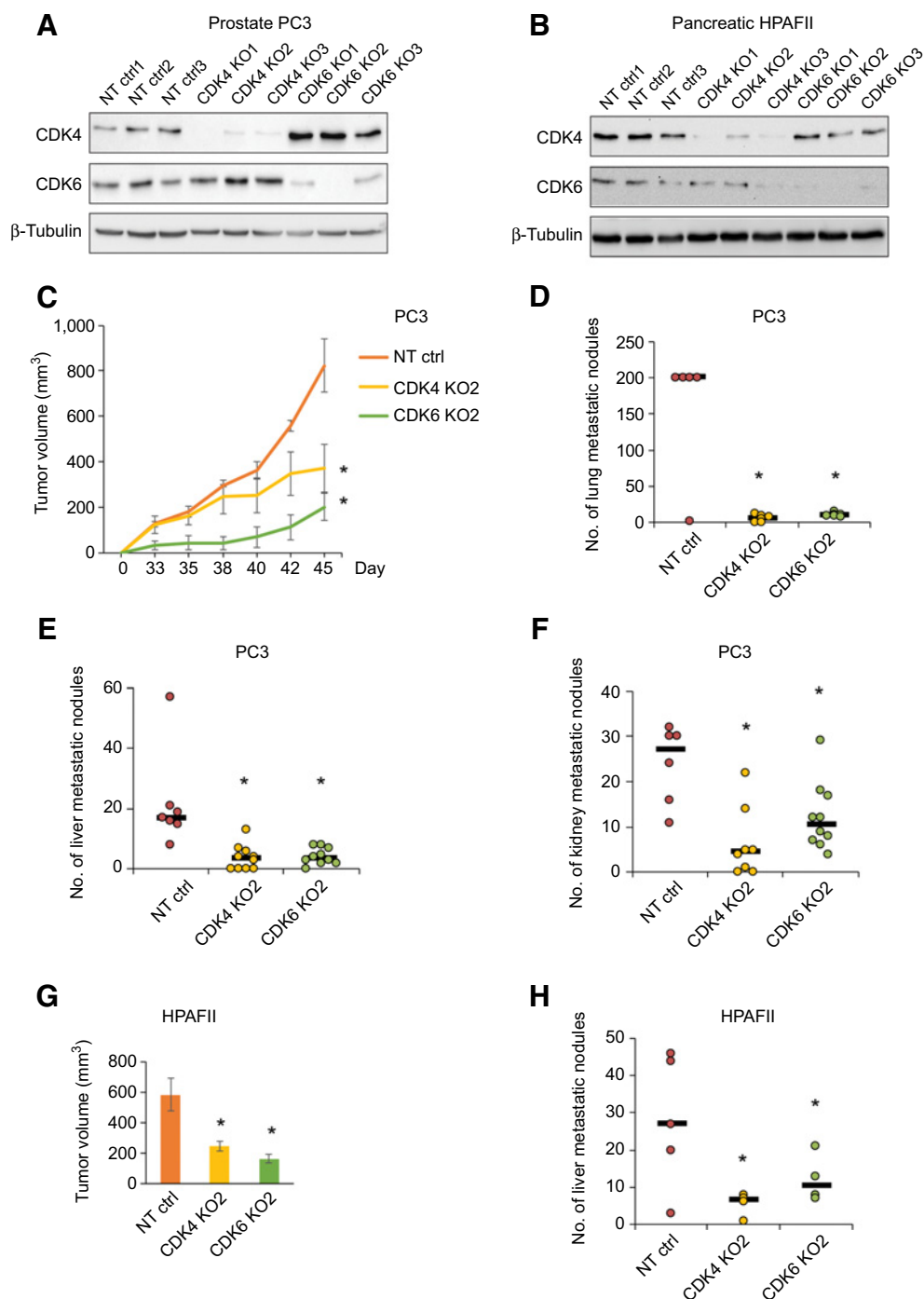
tissue (tumor cellularity) using hematoxylin and eosin and epithelial tumor cell marker (pan-cytokeratin) staining (Fig. 1H and I). Moreover, palbociclib treatment reduced lung metastatic nodules and the percentage of metastatic lesions in SUM159 and MDA intravenously injected NSG, respectively (Fig. 1J and K). Collectively, these findings provide direct evidence for a role of CDK4 and CDK6 on primary tumor formation and metastatic lung colonization in TNBC.

We then assessed whether the CDK4/6 effects on tumor growth and metastasis could extend to other solid tumor types using preclinical models of prostate and pancreatic cancer. CRISPR/Cas9-mediated CDK4/6 KOs in prostate (PC3) and pancreatic (HPAF-II) cancer cells was confirmed by immunoblotting (Figs. 2A and B). Primary prostate tumor growth was assessed following subcutaneous transplantation of the cancer cell line PC3 in NSG mice. As shown in Fig. 2C, knocking out CDK4 and CDK6 significantly prevented tumor growth. Furthermore, intravenous injection of CDK4 and CDK6 gRNA-infected PC3 cells led to a significant inhibition of the metastatic spread of the tumors to distant organs, including the lungs, liver, and kidneys (Fig. 2D–F). Using an orthotopic pancreas transplantation model, we also found that deletions of CDK4 and CDK6 in HPAF-II pancreatic cancer cells significantly reduced tumor volume (Fig. 2G). As liver is the primary site for pancreatic metastasis, we assessed the role of CDK4/6 on liver metastasis through intrasplenic transplantation of HPAF-II CDK4 KO and CDK6 KO cells. Both CDK4 and CDK6 KOs strongly reduced the number of liver metastatic nodules when compared with control cells in animals (Fig. 2H). Altogether, our results define CDK4/6 as potent regulators of tumor growth and metastatic process in various types of solid tumors, highlighting CDK4/6 as important druggable targets for patients with metastatic cancer.

CDK4 and CDK6 regulate distinct transcriptomes

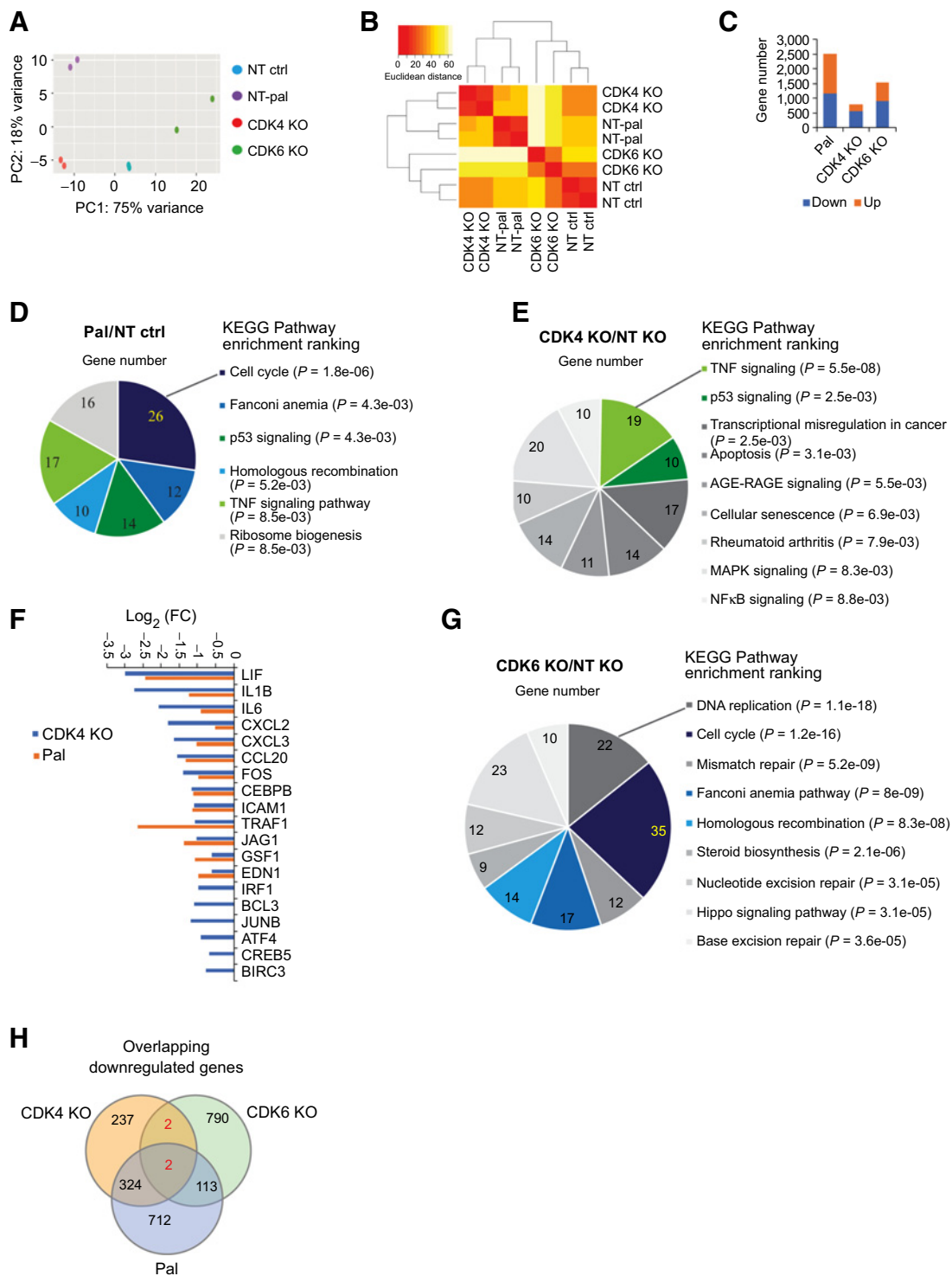
To gain further insight into the mechanisms by which CDK4 and CDK6 regulate primary tumor growth and metastasis, we performed transcriptomic profiling of CDK4 and CDK6 KO TNBC cells using RNA-seq. We also compared the transcriptomic profiles from CDK4/6 KO cells to inhibition of their kinase activity by palbociclib treatment. As shown in Fig. 3A and B, principal component analysis and unsupervised hierarchical clustering of the RNA-seq data revealed a tight clustering among biological replicates in the same conditions. Treatment of SUM159 cells with 100 nmol/L palbociclib for 24 hours altered expression (FDR < 0.05; FC > 1.5, < -1.5) of over 2,514 genes (1,363 up- and 1,151 downregulated genes), whereas the CDK4 and CDK6 KOs resulted in altered expression of 801 (236 up- and 565 down) and 1,527 (620 up- and 907 down) genes, respectively (Fig. 3C). To further analyze CDK4/6 KOs and palbociclib-regulated transcriptional programs, we performed pathway enrichment analysis of these gene sets (30). We focused on downregulated genes, as no enriched pathways were observed when using upregulated gene sets. As expected, the cell cycle emerged as the top enriched pathway for palbociclib-downregulated genes (Fig. 3D). In addition, other pathways involved in DNA repair process [Fanconi anemia and homologous recombination (HR)], p53 signaling, TNF signaling, and ribosome biogenesis were also ranked as significant (Figure 3D). Downregulated genes in CDK4 KO cells predominantly showed enrichment of the TNF signaling pathway, which contains many proinflammatory cytokines and chemokines (Fig. 3E and F). The TNF pathway and cytokines also overlapped in the palbociclib-regulated enrichment (Fig. 3E and F). Strikingly, CDK6 KO cells displayed a distinct pathway enrichment profile compared with the CDK4 KO cells, with top ranking downregulated genes being involved in DNA replication, cell cycle, and DNA repair pathways (including mismatch repair,

Distinct Roles for CDK4/6 in Cancer

**Figure 2.**

CDK4 and CDK6 CRISPR-KO impair primary tumor growth and distant metastasis in prostate and pancreatic cancer cells. **A** and **B**, Knockout efficiencies of the CDK4 and CDK6 KOs were assessed by immunoblotting in PC3 and HPAFII cells. **C**, Primary tumor growth was assessed following subcutaneous transplantation of PC3 KO cells in NSG mice ($n = 5$). **D-F**, NT, CDK4, and CDK6 KO PC3 cells were injected intravenously in NSG mice ($n = 6-10$ mice per group) and the number of metastatic nodules were quantified in lung (**D**), liver (**E**), and kidney (**F**) tissues. The midlines show median values. **G**, CDK4 and CDK6 KO HPAF-II cells were xenografted through orthotopic pancreatic transplantation in NSG mice ($n = 4$ mice per group). After 22 days, primary pancreatic tumors were collected for tumor volume measurement. **H**, Liver metastasis was monitored following intrasplenic injections of CDK4 and CDK6 KO HPAF-II pancreatic cancer cells. Metastatic nodules in liver were counted and are represented as dot plots for individual mice. The midlines show median value. All data are mean \pm SEM from three biological replicates unless otherwise stated. *, $P < 0.05$ by Student t test.

Dai et al.

**Figure 3.**

CDK4 and CDK6 regulate distinct transcriptomes. RNA-seq was performed in NT, CDK4, and CDK6 KO SUM159 cells as well as in palbociclib (pal)-treated conditions. **A** and **B**, Visualization of principal component analyses plot (**A**) and unsupervised clustering (**B**) analyses is presented for two biological replicates for each condition. **C**, Differential RNA-seq analyses comparing palbociclib-treated versus vehicle-treated NT SUM159, CDK4-KO versus NT, and CDK6-KO versus NT SUM159. Number of significantly up-/downregulated genes ($FC > 1.5$, < -1.5 ; $FDR < 0.05$) are shown. **D**, Kyoto Encyclopedia of Genes and Genomes (KEGG) pathway enrichment analysis using downregulated genes from palbociclib-treated versus vehicle-treated condition in NT SUM159 shows the number of genes in all significantly ranked pathways. **E**, KEGG pathway enrichment analysis of downregulated genes from CDK4-KO versus NT condition shows the number of genes in all significantly ranked pathways. **F**, RNA-seq Log₂ (FC) value for TNF signaling pathway-enriched genes in palbociclib and CDK4-KO targets. **G**, KEGG pathway enrichment analysis using downregulated genes from CDK6-KO versus NT condition shows the number of genes in all significantly ranked pathways. **H**, Venn diagram of overlapping differentially expressed genes between the CDK4 and CDK6 KOs and palbociclib treatment conditions.

Distinct Roles for CDK4/6 in Cancer

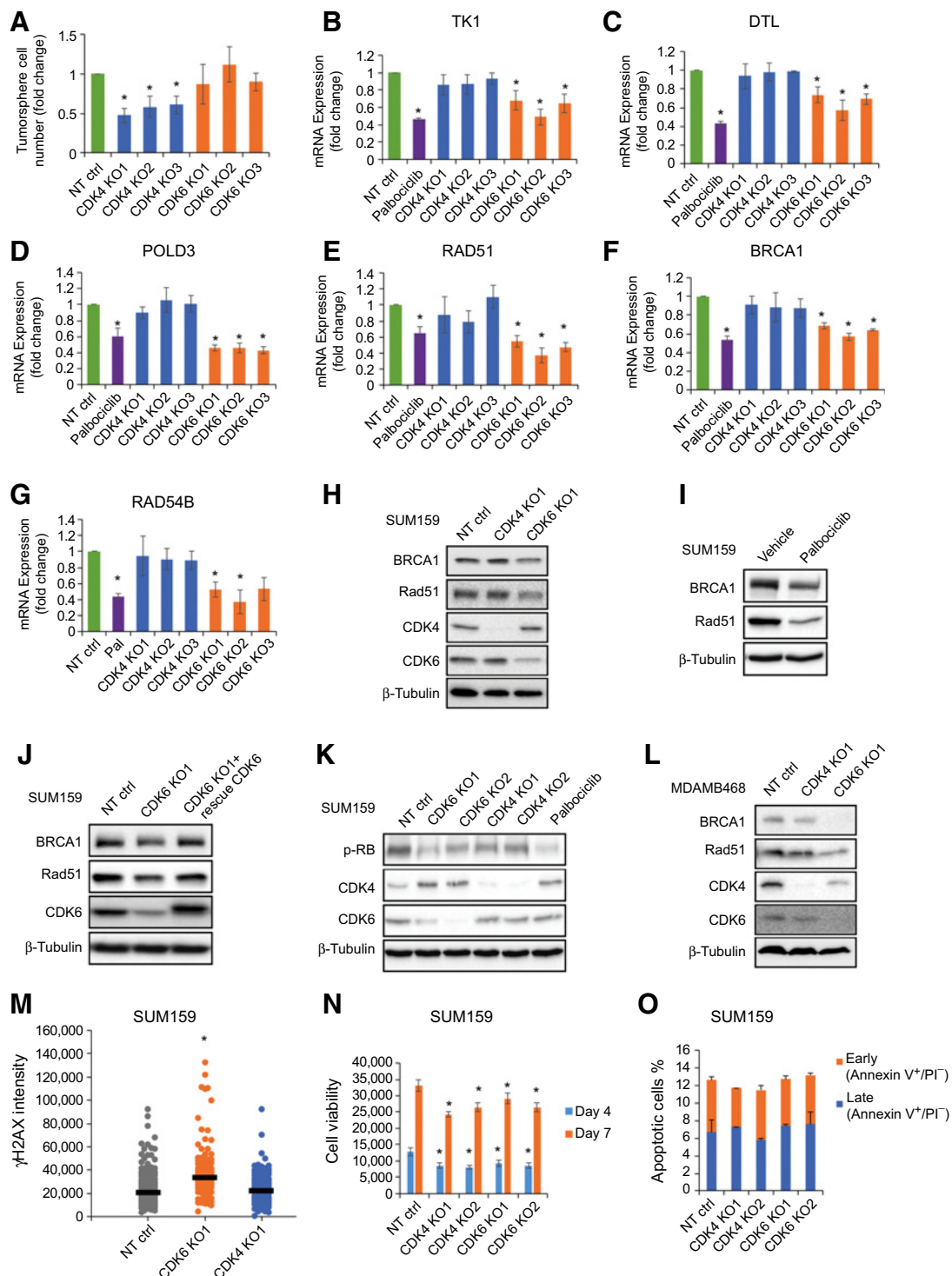
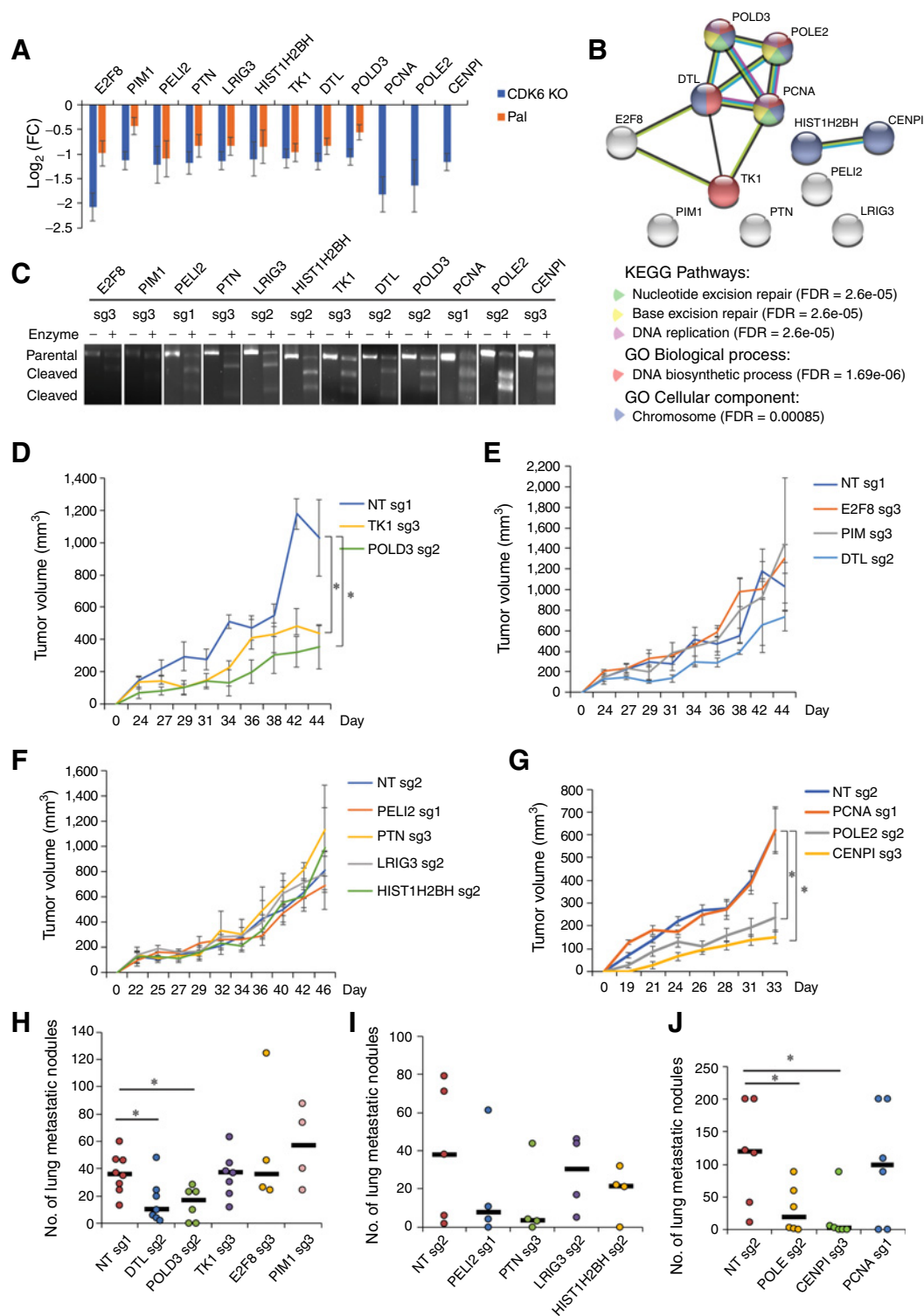


Figure 4.

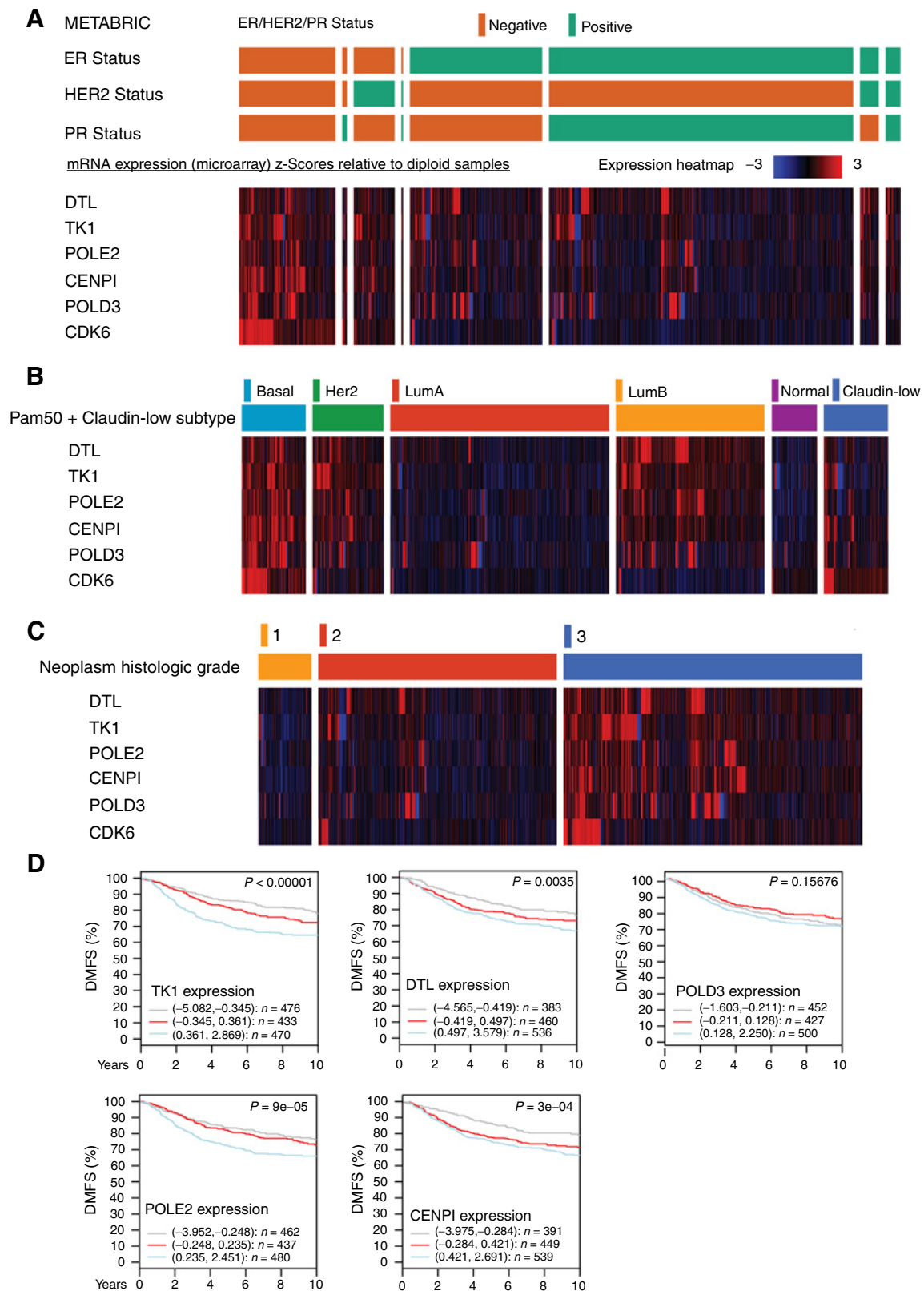
CDK6 regulates expression of the HR DNA repair pathway in TNBC cells. **A**, Tumorsphere cell numbers were quantified from NT, CDK4 KO, CDK6 KO SUM159 cells. **B-G**, mRNA expression of DNA replication (TK1, DTL, POLD3) and HR repair genes (*Rad51*, *BRCA1*, *Rad54B*) was measured by RT-PCR in NT, CDK4 KO, and CDK6 KO SUM159 cells. **H**, Immunoblotting of the indicated antibodies in NT, CDK4/6 KO SUM159 cells. **I**, Immunoblotting of the indicated antibodies in SUM159 treated with vehicle and 100 nmol/L palbociclib for 24 hours. **J**, Immunoblotting of the indicated antibodies in NT and CDK6 KO SUM159 cells as well as CDK6 KO cells overexpressed HA-CDK6 cDNA. **K**, Immunoblotting of the indicated antibodies in NT, CDK4/6 KO SUM159 cells as well as cells treated with palbociclib. **L**, Immunoblotting of the indicated antibodies in NT, CDK4/6 KO MDAMB468 cells. **M**, Immunofluorescent intensity of γ H2AX in NT, CDK4/6 KO SUM159 cells. **N**, Cell viability was quantified by Prestoblue staining in NT, CDK4/6 KO SUM159 cells. **O**, Apoptotic cells were quantified by Annexin V/PI staining in NT, CDK4/6 KO SUM159 cells. All data are mean \pm SEM from three biological replicates unless otherwise stated. *, $P < 0.05$ by Student *t* test.

Dai et al.

**Figure 5.**

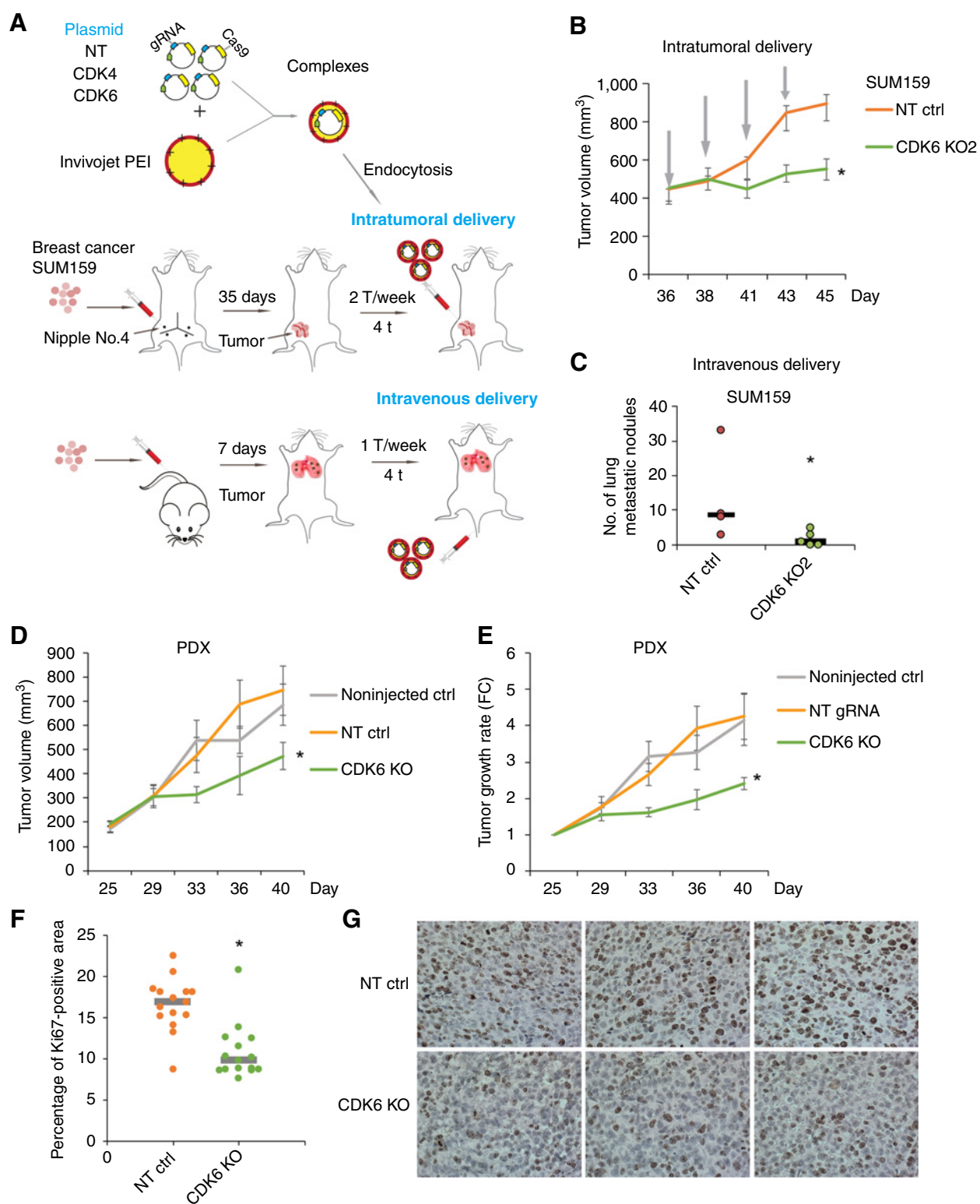
CDK6-regulated DNA replicative genes facilitate mammary tumor growth and metastatic colonization *in vivo*. **A**, RNA-seq Log₂ (FC) value for CDK6-targeted genes in response to palbociclib. **B**, STRING network visualization of 12 CDK6 target genes. **C**, Gene modification of specific gRNAs targeting distinct genomic sites on each gene were assessed by using genomic cleavage assays. **D–G**, gRNAs targeting the 12 CDK6 target genes in SUM159 cells were xenografted in NSG mice ($n = 5$ per group) through orthotopic mammary fat pad transplantation and primary tumor growth was assessed by measuring tumor volume. **H–J**, SUM159 cells knocked out individually for each of the 12 genes were injected intravenously in NSG mice to assess for metastasis. Lungs were collected and fixed in Bouin solution and metastatic nodules counted. Data are represented as dot plot for individual mice. The midlines show median value. All data are mean \pm SEM from three biological replicates unless otherwise stated. *, $P < 0.05$ by Student *t* test.

Distinct Roles for CDK4/6 in Cancer

**Figure 6.**

Clinical outcomes of CDK6-regulated DNA replication/repair genes. **A-C**, mRNA expression of CDK6 and its five DNA replication targets (TK1, DTL, POLD3, POLE2, CENPI) in 2,509 primary breast tumors using METABRIC dataset. The heatmaps of these patients categorized into TNBCs and non-TNBCs (**A**); different breast cancer subtypes (**B**) including basal-like, HER2⁺, luminal A, luminal B, normal-like, and claudin-low tumor tissues; tumor grades (**C**). **D**, Kaplan-Meier survival analysis of five CDK6 targets in distant metastasis-free survival (DMFS) using GOBO gene set analysis. Number of patients with breast cancer at risk with high (blue line), median (red line), low expression (gray line) of five genes.

Dai et al.

**Figure 7.**

In vivo delivery of a CRISPR/Cas9/anti-CDK6 gRNA efficiently prevents mammary tumor growth and metastatic colonization in a cell- and patient-derived xenograft model. **A**, Experimental procedure for CDK6 genomic deletion on a preclinical model of preestablished mammary tumors and metastatic lesions using a CRISPR/Cas9-based *in vivo* gene therapy delivery system. **B**, SUM159 breast cancer cells were transplanted into the mammary fat pad of NSG mice ($n = 5$ per group) and tumors allowed to develop for 35 days. (Continued on the following page.)

homologous recombination repair, and nucleotide/base excision repair; Fig. 3G). Some of the CDK6-regulated pathways (cell cycle, Fanconi anemia, and homologous recombination repair) were also regulated by palbociclib. The distinct transcriptomic regulation by CDK4 and CDK6 was further confirmed by the lack of overlapping gene sets, as only a few genes were commonly regulated by both CDK4 and CDK6 (Fig. 3H). Together, comprehensive transcriptomic analysis uncovered distinct signaling pathways and downstream targets for CDK4 and CDK6 in TNBC, suggesting their potential role in facilitating CDK4/6-mediated cancer growth and progression.

CDK6 regulates expression of the HR DNA repair pathway in TNBC cells

The CDK4-regulated proinflammatory cytokines and chemokines within the TNF α pathway are produced by tumor cells and have been well characterized as inducers of CSC self-renewal and distant metastasis in cancer (18, 31). Moreover, we previously showed that CDK4, but not CDK6, has a specific effect on the regulation of CSC self-renewal (18). Interestingly, we found that these effects on cancer stemness are CDK4 specific. Indeed, as shown in Fig. 4A, while CDK4 KO led to a marked decrease in tumorsphere formation, the CDK6 KO did not affect CSC numbers. In contrast to CDK4, CDK6 mainly targets DNA replication and repair, suggesting these pathways play important roles in regulating tumor growth and metastasis. To further demonstrate the specificity of CDK6 function on DNA replication and repair target gene expression, we examined the effect of CDK4 and CDK6 deletion on DNA replication (TK1, DTL, POLD3) and HR repair (*Rad51*, *BRCA1*, *Rad54B*) genes. As shown in Fig. 4B–G, all CDK6 target gene expressions were decreased by CDK6 KO and palbociclib, but remained unchanged in the CDK4 KOs, confirming the specificity of the downstream DNA replication and repair target gene for CDK6. Furthermore, these results highlighted potential new functions for CDK6-regulated HR DNA repair in cancer progression. To further investigate this, we first examined the CDK6 KO effects on the protein levels of two HR pathway main regulators, BRCA1 and Rad51. As shown in Fig. 4H and I, blocking CDK6 expression (KO) or activity (palbociclib), efficiently reduced BRCA1 and Rad51 protein expression in SUM159 cells, while the CDK4 KO showed no effect. To ensure that these effects were CDK6-specific, we overexpressed an HA-tagged CDK6 cDNA in the CDK6 KO background. As shown in Fig. 4J, rescuing CDK6 expression in the KO cells potently restored both BRCA1 and Rad51 protein expression levels to what observed in control cells, confirming the specificity of the CDK6 effects.

We next examined the RB phosphorylation state under CDK4/6 KO and pharmacologic inhibition (palbociclib). As expected, CDK4 KO, CDK6 KO and CDK4/6i all significantly reduced RB phosphorylation levels in RB⁺ SUM159 cells (Fig. 4K), palbociclib being the most efficient, with no significant difference between the CDK4 and CDK6 KOs. To then address whether the CDK6 effects on DNA repair are RB dependent, we deleted CDK6 expression in RB-deficient MDA-MB-468 cells and examined CDK6 DNA repair target gene expression (*BRCA1* and *Rad51*). Interestingly, the CDK6 KO also reduced

expression of DNA repair proteins (*BRCA1* and *Rad51*) in RB-deficient cells (Fig. 4L), suggesting that the CDK6 effects on DNA repair are RB-independent. We also found the specific inhibition of CDK6 to increase DNA damage, as measured by phosphorylation intensity of the DNA damage marker (γ H2AX; Fig. 4M). This was followed by a decrease in cell proliferation but no change in apoptosis (Fig. 4N and O). Together, these data indicate that CDK6 gene ablation inhibits the HR DNA repair pathway, increases DNA damage and further decreases the tumor proliferation, resulting in reduced tumor growth and metastatic colonization of the lungs.

CDK6-regulated DNA replicative genes facilitate mammary tumor growth and metastatic colonization *in vivo*

To further examine whether CDK6-regulated DNA replication and repair can modulate tumor formation and metastasis *in vivo*, we validated the top 12 CDK6-regulated target genes. Indeed, when analyzing the gene amplification and p53 mutation status of the CDK6 targets across pan-cancer TCGA, we found that the top 12 targets were significantly amplified in patients with breast cancer and frequently associated with p53 mutations (Supplementary Fig. S2A and B). As shown in Fig. 5A, most of the CDK6-regulated genes (*DTL*, *TK1*, *POLD3*, *HIST1H2BH*, *E2F8*, *PTN*, *LRIG3*, *PELI2*, *PIMI1*) are also downregulated by palbociclib treatment. Of these, gene network analysis showed that five (*TK1*, *DTL*, *POLD3*, *PCNA*, *POLE2*) are well-known regulators of DNA replication and repair, each controlling specific steps of this tightly regulated sequential process (Fig. 5B). All 12 genes were individually knocked out in SUM159 TNBC cells using lentiviral CRISPR/Cas9 with three specific gRNAs for each target. Indel mutation efficiency was assessed using a genomic cleavage assay (Fig. 5C). SUM159 TNBC cells harboring the highest indel efficiency for each gene were then transplanted into the mammary fat pad of NSG mice and injected intravenously into the tail vein to assess for tumor formation and metastatic colonization, respectively. Out of 12, five genes showed a significant effect on either tumor growth or lung metastatic lesion. Specifically, we found that *TK1*, *POLD3*, *POLE2*, *CENPI* KOs significantly reduced primary mammary tumor growth (Fig. 5D–G), while *DTL*, *POLD3*, *POLE2*, *CENPI* KOs significantly impaired breast cancer cells metastatic colonization to the lungs (Fig. 5H–J). Three genes (*POLD3*, *POLE2*, *CENPI*) affected both processes. Importantly, five of these functionally identified genes are essential to the DNA replication/repair processes and chromosome segregation, demonstrating that CDK6-regulated DNA replication and DNA repair represents a predominant pathway in regulating TNBC tumor growth and metastatic process.

Among the different breast cancer molecular subtypes, TNBC has the lowest therapeutic options and survival outcomes. TNBC exhibit frequent recurrence, poor outcomes and have a very high-grade status and metastatic potential (32). The heterogenous nature of TNBC makes it challenging to treat efficiently and therapeutic options are often limited to conventional therapy. Interestingly, analysis of 550 patients with TNBC from two combined METABRIC and TCGA

(Continued.) CRISPR/Cas9 plasmid DNA constructs expressing individual gRNAs, either NT or targeting CDK6, were then combined with a polymer-based lipid reagent InvivoJet PEI before being delivered through direct intratumoral injection. Primary mammary tumor volume is presented. C, SUM159 cells were intravenously injected into NSG mice ($n = 5$ per group). Metastatic nodules in lung were counted following Bouin solution fixation and are represented as dot plot for individual mice. The midlines show median value. D and E, PDX model was subcutaneously transplanted into NSG mice ($n = 6$ per group). CRISPR/Cas9 plasmid DNA constructs expressing individual gRNAs, either NT or targeting CDK6, were delivered through direct intratumoral injection. Primary mammary tumor volume and individual tumor growth rate are shown. F and G, Quantification and representative images of Ki67 positive cells in PDX tumor tissues from both groups. All data are mean \pm SEM unless otherwise stated. *, $P < 0.05$ by Student t test.

Dai et al.

datasets revealed copy numbers of MYC (64%), PIK3CA (51%), and CDK6 (39%) are the most commonly gained/amplified genes across all five heterogeneous TNBC subtypes (33). To further understand the clinical impact of the five DNA replication/repair CDK6 targets in TNBC, we first compared their gene expression levels in different subtypes of breast cancer patient tissue samples as well as TNBC versus other non-TNBC molecular subtypes tissue samples in the cBioPortal datasets (34, 35). Using both METABRIC and TCGA datasets of 2,509 and 1,215 primary human breast tumors, we found that along with CDK6, all these genes were highly expressed in both TNBC tumors and basal like subtype compared with normal tissues and other subtypes (Fig. 6A and B; Supplementary Fig. S3A and S3B). Furthermore, we found overexpression of all five genes correlated with high tumor grade (Fig. 6C) with four genes also significantly correlating with poor distant metastatic survival outcome using cBioPortal and GOBO gene set analysis (Fig. 6D; Supplementary Fig. S3C; ref. 36). Thus, our data indicate that these CDK6-regulated DNA replication and repair genes could serve as prognostic biomarkers for high-grade tumors and poor clinical outcomes.

***In vivo* delivery of a CRISPR/CDK6 gRNA efficiently prevents mammary tumor growth and lung metastatic colonization**

We next evaluated whether specifically targeting CDK6 would represent a valuable option for new targeted therapy in TNBC. To this end, we performed CDK6 genomic deletions in clinically relevant models of preestablished mammary tumors and metastatic lesions using a CRISPR-based *in vivo* gene therapy delivery system. To evaluate primary tumor formation, SUM159 TNBC cells were first transplanted into the mammary fat pad of NSG mice and allowed to grow for 35 days to develop palpable tumors of approximately 500 mm³ in size. Specific CRISPR plasmid DNA constructs expressing single NT gRNAs or gRNAs targeting CDK6 were then combined with a polymer-based lipid reagent (*in vivo*-jetPEI) before being delivered through direct intratumoral injection of the preformed tumors (illustrated in Fig. 7A). The *in vivo*-jetPEI reagent has demonstrated high efficiency and stability in delivering nucleic acids *in vivo* and is currently being tested as a delivery agent for plasmid DNA/siRNA in preclinical and clinical trials (37). A CRISPR/NT gRNA was used as a negative control. Remarkably, repeated local, intratumoral delivery of the CRISPR/CDK6 gRNA construct completely prevented further growth of established mammary tumors, contrary to the NT gRNA (Fig. 7B). We next explored the potential therapeutic value of this system against the development of secondary metastatic lesions. For this, SUM159 TNBC cells were inoculated in NSG mice through intravenous injections in the tail vein to allow for the seeding of the cancer cells to the lungs and the development of lung metastatic lesions. One week postinjection, CRISPR/gRNAs targeting CDK6 or NT combined with *in vivo*-jetPEI were administered intravenously at weekly intervals for another four weeks. Lung tissues were collected at the fifth week and assessed for the presence of metastatic nodules. Importantly, as shown in Fig. 7C, injection of the CRISPR/CDK6 gRNA significantly decreased the number of lung metastatic nodules compared with the NT gRNA delivery control group.

To further investigate the clinical relevance of our *in vivo* delivery of CRISPR/CDK6 gRNA treatment for patients with TNBC, we used a TNBC PDX model, which was established from a grade 3 metastatic invasive ductal carcinoma. PDX tumors were expanded to three groups (noninjected control, NT gRNA, and CDK6 gRNA) by subcutaneous transplantation in NSG mice. Animals were then injected with or without gRNAs through intratumor injections (2 × per week for two weeks). Excitingly, while NT gRNA showed no effect compared

with the noninjected group, the CDK6 gRNA strongly and significantly reduced both tumor volume and tumor growth rates of the individual transplanted mice (Fig. 7D and E). Importantly, we also examined the *in vivo* proliferation index (Ki67) by IHC staining of control PDX tumors versus tumors delivered with NT and CDK6 KO. Our result showed reduced Ki67-positive cell numbers in CDK6 CRISPR/gRNA injected tumors compared with tumors injected with a NT gRNA, indicative of a reduced rate of cell proliferation *in vivo* (Fig. 7F and G). Taken together, these results highlight a critical role played by CDK6 on solid tumor formation and progression and define a novel potential therapeutic approach that can efficiently prevent the growth and spread of established tumors in TNBC.

Discussion

In this study, we made use of CRISPR-mediated gene knockout and pharmacologic inhibition approaches to address the function of CDK4 and CDK6 towards tumor growth and progression in multiple types of solid tumors. Our comprehensive transcriptomic analysis and functional characterization of large sets of downstream targets in patients' datasets and *in vivo* models uncovered distinct signaling pathways and downstream targets for these two kinases. While CDK4 regulates inflammatory cytokine signaling, CDK6 mainly controls DNA replication and DNA repair processes. Our results further highlight novel important functions for CDK6 in regulating DNA repair in the context of cancer formation and progression and show that silencing CDK6, but not CDK4 results in a defective DNA repair and increased DNA damage. In-depth analysis further revealed that multiple CDK6 DNA replication/repair genes are not only associated with cancer subtype, grades, and poor clinical outcomes, but also facilitate primary tumor growth and metastasis. Together, these results highlight the prominent role played by CDK6-mediated DNA repair in controlling tumor initiation and cancer progression.

The role and contribution of CDK4/6 to cancer progression and metastasis is not well-characterized. Here, using CRISPR-KO models, we discovered that CDK4 and CDK6 are required to drive tumor growth and metastatic process in several types of solid tumors, including breast, prostate, and pancreatic cancer. Importantly, pharmacologic CDK4/6i, using palbociclib reduced both tumor growth and lung metastatic colonization in TNBCs. In particular, we found CDK6 and downstream DNA replication and repair target genes to play a central role in these processes. Of note, these patients with cancer frequently develop recurrent and metastatic disease and are missing an effective targeted therapy, leading to very low survival rates. We showed here that *in vivo* delivery of a CRISPR/CDK6 cDNA construct combined with the *in vivo*-jetPEI polymer efficiently halted the continuous growth and spread of preestablished mammary tumor and metastasis in TNBC. Thus, our findings provide a strong rationale for targeting CDK6 as a potential therapy for patients with metastatic cancer. These results also indicate that the CDK6 oncogenic functions are not limited to blood cancers (14), but also extend to solid tumors. Of note, it is important to mention that the immunodeficient NSG mice models used in the study do not take into account any potential role played by the tumor immune microenvironment in the mediation of the CDK4/6 effects on tumor progression. Thus, it will be interesting in future studies to also investigate the CDK4/6 and DNA repair functions using immunocompetent mice models to further address the contribution of the tumor microenvironment.

Our genomic profiling studies revealed that CDK4 and CDK6 have very distinct transcriptomes, with CDK4 predominantly regulating proinflammatory signaling and CDK6 controlling DNA replication/

repair pathways. While the CDK4 downstream targets are well-known oncogenic markers, the role or function of the CDK6-regulated DNA replication and DNA repair target genes remain largely uncharacterized in the context of tumor growth and progression. Of note, TNBC is commonly associated with a high DNA replicative rate and a largely instable genome (38). Moreover, CDK6 KO and palbociclib inhibition specifically reduced essential HR protein BRCA1 and RAD51. This leads to increased level of DNA damage marker γ H2AX and reduced cell viability. Accordingly, our study indicates that CDK6-regulated DNA replication/repair is a potential prevailing oncogenic pathway in TNBC tumor growth and metastatic colonization. Using *in vivo* preclinical models of breast cancer, we identified five DNA replicative genes (*TK1*, *DTL*, *POLD3*, *POLE2*, *CENPI*), which are critical for tumor growth and progression. Thymidine kinase 1 *TK1* is an important enzyme for nucleotide metabolism during DNA synthesis (39). Denticleless protein homolog *DTL* is a substrate-specific adapter for CRL4 E3 ubiquitin-protein ligase complex that mediates degradation of cell cycle and DNA replication proteins (40). The two DNA polymerases, *POLE2* and *POLD3*, function as leading and lagging strand DNA synthesis and repair processes (41). *CENPI*, a centromere protein in the CENPA-NAC complex, is critical for accurate chromosome alignment and segregation during mitotic division (42). On the basis of our data, these DNA replication and repair genes could serve as prognostic biomarkers for high-grade tumors and poor clinical outcomes.

Our data also show that *DTL*, *POLD3*, *POLE2*, and *CENPI* are not only essential regulators of metastatic colonization but also frequently amplified in patients metastatic breast cancer, suggesting that they may serve as useful biomarkers for disease progression and late-stage metastasis. *POLD3/POLE2* and *CENPI* are essential for DNA replication and chromosome segregation. In addition to DNA synthesis, *POLD3/POLE2* are also critical for DNA fidelity and is potentially associated with chromatin instability (43). We found expression of these genes to be decreased in the CDK6 KO, suggesting that pharmacological inhibition of CDK6 results in defective DNA repair. Because TNBCs exhibit high DNA replicative activity, the use of such CDK6 inhibitors could prove useful and potentially synergies with DNA repair inhibitors to trigger synthetic lethality in these aggressive tumors. This will provide greater clinical benefits for CDK6 inhibitors for patients with TNBC and should be explored in new clinical trial settings.

While encouraging progress has been made in recent years in the treatment of early carcinoma, the cancer death burden still mostly rests on secondary metastatic tumors that have spread from the initial site (44). The longstanding goal of targeting CDK4/6 as an anticancer therapeutic has recently gained a lot of attention and is now considered a first-line treatment for patients with breast cancer. Several CDK4/6 inhibitors are currently undergoing clinical trials for different types of advanced or metastatic cancer including breast cancer, glioblastoma, leukemia, and pancreatic carcinoma (45–47). While these studies have demonstrated the clinical relevance of using the CDK4/6 axis for metastatic breast cancer treatment, the molecular mechanisms by which these kinases exert their effects to drive and further propagate tumor metastasis have not yet been characterized. Experimental

evidence using gene-deficient mice models have demonstrated that CDK4 and CDK6 have redundant function in normal development (6, 13, 48). In our study, we demonstrated that CDK4 and CDK6 exert separate functions in facilitating tumor growth and expansion, suggesting a multifaceted benefit can be gleaned by targeting CDK4 and CDK6 in metastatic cancers.

Several clinical trials have reported unexpected outcomes when using CDK4/6 inhibitors in patients with breast cancer. Despite significantly improving progression-free survival in the majority of patients, when used in combination with aromatase inhibitors (49), one third of patients with ER⁺ breast cancer and most patients with TNBC did not respond to the inhibition of CDK4/6. This ultimately discouraged further investigation of the clinical benefits of palbociclib in patients with TNBC. It is worth noting that the positive response to palbociclib treatment was unrelated to the degree of endocrine resistance, hormone receptor expression level, and PIK3CA mutational status (frequent mutation in breast cancer) in patients with breast cancer, highlighting the need for predictive biomarkers for palbociclib sensitivity in TNBC (46). Of note, serum level of thymidine kinase *TK1* has been identified a predictive biomarker for patients with early-stage ER⁺ breast cancer when receiving palbociclib treatment (50). Interestingly, our study revealed that palbociclib and CDK6 specifically regulate *TK1* gene expression as well as two other genes *DTL/POLD3* in TNBC. We also found that these genes facilitate primary tumor growth and metastatic colonization, highlighting them as potential biomarkers for selecting patients with TNBC that could receive CDK4/6 inhibitor treatment.

Authors' Disclosures

J.-J. Lebrun reports grants from Canadian Institutes for Health Research during the conduct of the study. No disclosures were reported by the other authors.

Authors' Contributions

M. Dai: Conceptualization, formal analysis, validation, investigation, visualization, methodology, writing-original draft, writing-review and editing. **J. Boudreau:** Validation, investigation, methodology. **N. Wang:** Formal analysis, validation, investigation, methodology. **S. Poulet:** Validation, investigation, writing-original draft, writing-review and editing. **G. Daliah:** Validation, investigation, methodology. **G. Yan:** Formal analysis, validation, investigation. **A. Moamer:** Validation, investigation. **S.A. Burgos:** Validation, investigation, writing-original draft, writing-review and editing. **S. Sabri:** Validation, investigation. **S. Ali:** Formal analysis, investigation, writing-original draft, writing-review and editing. **J.-J. Lebrun:** Conceptualization, resources, formal analysis, supervision, funding acquisition, visualization, writing-original draft, project administration, writing-review and editing.

Acknowledgments

J.-J. Lebrun received Canadian Institutes for Health Research (CIHR) grant 8117.

The costs of publication of this article were defrayed in part by the payment of page charges. This article must therefore be hereby marked *advertisement* in accordance with 18 U.S.C. Section 1734 solely to indicate this fact.

Received June 22, 2020; revised November 3, 2020; accepted December 21, 2020; published first December 28, 2020.

References

- Sherr CJ. G1 phase progression: cycling on cue. *Cell* 1994;79:551–5.
- Kato J, Matsushima H, Hiebert SW, Ewen ME, Sherr CJ. Direct binding of cyclin D to the retinoblastoma gene product (pRb) and pRb phosphorylation by the cyclin D-dependent kinase CDK4. *Genes Dev* 1993;7:331–42.
- Blow JJ, Ge XQ, Jackson DA. How dormant origins promote complete genome replication. *Trends Biochem Sci* 2011;36:405–14.
- Kotsantis P, Petermann E, Boulton SJ. Mechanisms of oncogene-induced replication stress: jigsaw falling into place. *Cancer Discov* 2018;8:537–55.

Dai et al.

5. Kozar K, Ciemerych MA, Rebel VI, Shigematsu H, Zagodzón A, Sicinska E, et al. Mouse development and cell proliferation in the absence of D-cyclins. *Cell* 2004;118:477–91.
6. Malumbres M, Sotillo R, Santamaria D, Galan J, Cerezo A, Ortega S, et al. Mammalian cells cycle without the D-type cyclin-dependent kinases Cdk4 and Cdk6. *Cell* 2004;118:493–504.
7. Arnold A, Papanikolaou A. Cyclin D1 in breast cancer pathogenesis. *J Clin Oncol* 2005;23:4215–24.
8. Yu Q, Sicinska E, Geng Y, Ahnstrom M, Zagodzón A, Kong Y, et al. Requirement for CDK4 kinase function in breast cancer. *Cancer Cell* 2006;9:23–32.
9. Massague J. G1 cell-cycle control and cancer. *Nature* 2004;432:298–306.
10. Puyol M, Martin A, Dubus P, Mulero F, Pizcueta P, Khan G, et al. A synthetic lethal interaction between K-Ras oncogenes and Cdk4 unveils a therapeutic strategy for non-small cell lung carcinoma. *Cancer Cell* 2010;18:63–73.
11. Lee RJ, Albanese C, Fu M, D'Amico M, Lin B, Watanabe G, et al. Cyclin D1 is required for transformation by activated Neu and is induced through an E2F-dependent signaling pathway. *Mol Cell Biol* 2000;20:672–83.
12. Yu Q, Geng Y, Sicinski P. Specific protection against breast cancers by cyclin D1 ablation. *Nature* 2001;411:1017–21.
13. Ortega S, Malumbres M, Barbacid M. Cyclin D-dependent kinases, INK4 inhibitors and cancer. *Biochim Biophys Acta* 2002;1602:73–87.
14. Kollmann K, Heller G, Schneckelthner C, Warsch W, Scheicher R, Ott RG, et al. A kinase-independent function of CDK6 links the cell cycle to tumor angiogenesis. *Cancer Cell* 2013;24:167–81.
15. Anders L, Ke N, Hydbring P, Choi YJ, Widlund HR, Chick JM, et al. A systematic screen for CDK4/6 substrates links FOXM1 phosphorylation to senescence suppression in cancer cells. *Cancer Cell* 2011;20:620–34.
16. Dai M, Al-Odaini AA, Fils-Aime N, Villatoro MA, Guo J, Arakelian A, et al. Cyclin D1 cooperates with p21 to regulate TGFbeta-mediated breast cancer cell migration and tumor local invasion. *Breast Cancer Res* 2013;15:R49.
17. Fuste NP, Fernandez-Hernandez R, Cemeli T, Mirantes C, Pedraza N, Rafel M, et al. Cytoplasmic cyclin D1 regulates cell invasion and metastasis through the phosphorylation of paxillin. *Nat Commun* 2016;7:11581.
18. Dai M, Zhang C, Ali A, Hong X, Tian J, Lo C, et al. CDK4 regulates cancer stemness and is a novel therapeutic target for triple-negative breast cancer. *Sci Rep* 2016;6:35383.
19. Liu T, Yu J, Deng M, Yin Y, Zhang H, Luo K, et al. CDK4/6-dependent activation of DUB3 regulates cancer metastasis through SNAIL1. *Nat Commun* 2017;8:13923.
20. Alvarez-Fernandez M, Malumbres M. Mechanisms of Sensitivity and Resistance to CDK4/6 Inhibition. *Cancer Cell* 2020;37:514–29.
21. DeMichele A, Clark AS, Tan KS, Heitjan DF, Gramlich K, Gallagher M, et al. CDK 4/6 inhibitor palbociclib (PD0332991) in Rb+ advanced breast cancer: phase II activity, safety, and predictive biomarker assessment. *Clin Cancer Res* 2015;21:995–1001.
22. Sanjana NE, Shalem O, Zhang F. Improved vectors and genome-wide libraries for CRISPR screening. *Nat Methods* 2014;11:783–4.
23. van den Heuvel S, Harlow E. Distinct roles for cyclin-dependent kinases in cell cycle control. *Science* 1993;262:2050–4.
24. Tuominen VJ, Ruotoistenmaki S, Viitanen A, Jumppanen M, Isola J. ImmunoRatio: a publicly available web application for quantitative image analysis of estrogen receptor (ER), progesterone receptor (PR), and Ki-67. *Breast Cancer Res* 2010;12:R56.
25. Kim D, Langmead B, Salzberg SL. HISAT: a fast spliced aligner with low memory requirements. *Nat Methods* 2015;12:357–60.
26. Li H, Handsaker B, Wysoker A, Fennell T, Ruan J, Homer N, et al. The sequence alignment/Map format and SAMtools. *Bioinformatics* 2009;25:2078–9.
27. Zerbino DR, Achuthan P, Akanni W, Amodè MR, Barrell D, Bhaj J, et al. Ensembl 2018. *Nucleic Acids Res* 2018;46:D754–D61.
28. Anders S, Pyl PT, Huber W. HTSeq—a Python framework to work with high-throughput sequencing data. *Bioinformatics* 2015;31:166–9.
29. Love MI, Huber W, Anders S. Moderated estimation of fold change and dispersion for RNA-seq data with DESeq2. *Genome Biol* 2014;15:550.
30. Kuleshov MV, Jones MR, Rouillard AD, Fernandez NF, Duan Q, Wang Z, et al. Enrichr: a comprehensive gene set enrichment analysis web server 2016 update. *Nucleic Acids Res* 2016;44:W90–7.
31. Mantovani A, Allavena P, Sica A, Balkwill F. Cancer-related inflammation. *Nature* 2008;454:436–44.
32. Lehmann BD, Bauer JA, Chen X, Sanders ME, Chakravarthy AB, Shyr Y, et al. Identification of human triple-negative breast cancer subtypes and preclinical models for selection of targeted therapies. *J Clin Invest* 2011;121:2750–67.
33. Bareche Y, Venet D, Ignatiadis M, Aftimos P, Piccart M, Rothe F, et al. Unravelling triple-negative breast cancer molecular heterogeneity using an integrative multiomic analysis. *Ann Oncol* 2018;29:895–902.
34. Cerami E, Gao J, Dogrusoz U, Gross BE, Sumer SO, Aksoy BA, et al. The cBio cancer genomics portal: an open platform for exploring multidimensional cancer genomics data. *Cancer Discov* 2012;2:401–4.
35. Gao J, Aksoy BA, Dogrusoz U, Dresdner G, Gross B, Sumer SO, et al. Integrative analysis of complex cancer genomics and clinical profiles using the cBioPortal. *Sci Signal* 2013;6:pl1.
36. Ringner M, Fredlund E, Hakkinen J, Borg A, Staaf J. GOBO: gene expression-based outcome for breast cancer online. *PLoS One* 2011;6:e17911.
37. Bhang HE, Gabrielson KL, Laterra J, Fisher PB, Pomper MG. Tumor-specific imaging through progression elevated gene-3 promoter-driven gene expression. *Nat Med* 2011;17:123–9.
38. Cancer Genome Atlas N. Comprehensive molecular portraits of human breast tumours. *Nature* 2012;490:61–70.
39. Ke PY, Chang ZF. Mitotic degradation of human thymidine kinase 1 is dependent on the anaphase-promoting complex/cyclosome-CDH1-mediated pathway. *Mol Cell Biol* 2004;24:514–26.
40. Panagopoulos A, Taraviras S, Nishitani H, Lygerou Z. CRL4(Cdt2): coupling genome stability to ubiquitination. *Trends Cell Biol* 2020;30:290–302.
41. Johnson RE, Klassen R, Prakash L, Prakash S. A Major Role of DNA Polymerase delta in Replication of Both the Leading and Lagging DNA Strands. *Mol Cell* 2015;59:163–75.
42. Matson DR, Stukenberg PT. CENP-I and Aurora B act as a molecular switch that ties RZZ/Mad1 recruitment to kinetochore attachment status. *J Cell Biol* 2014;205:541–54.
43. Bebenek A, Ziuzia-Graczyk I. Fidelity of DNA replication—a matter of proof-reading. *Curr Genet* 2018;64:985–96.
44. Gupta GP, Massague J. Cancer metastasis: building a framework. *Cell* 2006;127:679–95.
45. Guha M. Blockbuster dreams for Pfizer's CDK inhibitor. *Nat Biotechnol* 2013;31:187.
46. Cristofanilli M, Turner NC, Bondarenko I, Ro J, Im SA, Masuda N, et al. Fulvestrant plus palbociclib versus fulvestrant plus placebo for treatment of hormone-receptor-positive, HER2-negative metastatic breast cancer that progressed on previous endocrine therapy (PALOMA-3): final analysis of the multicentre, double-blind, phase 3 randomised controlled trial. *Lancet Oncol* 2016;17:425–39.
47. Finn RS, Martin M, Rugo HS, Jones S, Im SA, Gelmon K, et al. Palbociclib and letrozole in advanced breast cancer. *N Engl J Med* 2016;375:1925–36.
48. Zou X, Ray D, Aziyu A, Christov K, Boiko AD, Gudkov AV, et al. Cdk4 disruption renders primary mouse cells resistant to oncogenic transformation, leading to Arf/p53-independent senescence. *Genes & development* 2002;16:2923–34.
49. Turner NC, Ro J, André F, Loi S, Verma S, Iwata H, et al. Palbociclib in hormone-receptor-positive advanced breast cancer. *N Engl J Med* 2015;373:209–19.
50. Bagegni N, Thomas S, Liu N, Luo J, Hoog J, Northfelt DW, et al. Serum thymidine kinase 1 activity as a pharmacodynamic marker of cyclin-dependent kinase 4/6 inhibition in patients with early-stage breast cancer receiving neoadjuvant palbociclib. *Breast Cancer Res* 2017;19:123.

Cancer Research

The Journal of Cancer Research (1916–1930) | The American Journal of Cancer (1931–1940)

Differential Regulation of Cancer Progression by CDK4/6 Plays a Central Role in DNA Replication and Repair Pathways

Meiou Dai, Julien Boudreault, Ni Wang, et al.

Cancer Res 2021;81:1332-1346. Published OnlineFirst December 28, 2020.

Updated version	Access the most recent version of this article at: doi: 10.1158/0008-5472.CAN-20-2121
Supplementary Material	Access the most recent supplemental material at: http://cancerres.aacrjournals.org/content/suppl/2020/12/24/0008-5472.CAN-20-2121.DC1

Cited articles	This article cites 50 articles, 11 of which you can access for free at: http://cancerres.aacrjournals.org/content/81/5/1332.full#ref-list-1
-----------------------	--

E-mail alerts	Sign up to receive free email-alerts related to this article or journal.
Reprints and Subscriptions	To order reprints of this article or to subscribe to the journal, contact the AACR Publications Department at pubs@aacr.org .
Permissions	To request permission to re-use all or part of this article, use this link http://cancerres.aacrjournals.org/content/81/5/1332 . Click on "Request Permissions" which will take you to the Copyright Clearance Center's (CCC) Rightslink site.